Ion−Molecule Reactions and Fragmentation Patterns in Helium Nanodroplets†

Adrian Boatwright, Jay Jeffs, and Anthony J. Stace*

Department of Physical Chemistry, School of Chemistry, The University of Nottingham, University Park, Nottingham NG7 2RH, U.K.

Received: February 19, 2007; In Final Form: May 15, 2007

A study has been made of the ion chemistry of a series of small molecules that have been embedded in helium nanodroplets. In most instances, the molecules H_2O, SO_2, CO_2, CH_3OH, C_2H_5OH, C_3H_7OH, CH_3F, and CH_3Cl have been allowed to form clusters, and reactivity within these has been initiated through electron impact ionization. For two of the molecules studied, CF_2Cl_2 and CF_3I, reactivity is believed to originate from single molecules embedded in the droplets. Electron impact on the droplets is thought to first create a helium ion, and formation of molecular ions is then assumed to proceed via a charge hopping mechanism that propagates though the droplet and terminates with charge-transfer to a molecule or cluster. The chemistry exhibited by many of the cluster ions and at least one of the single molecular ions is very different from that observed for the same species in isolation. In most cases, reactivity appears to be dominated by high-energy bond breaking processes as opposed to, in the case of the clusters, ion−molecule reactions. Overall, charge-transfer from He^+ does not appear to be a "soft" ionization mechanism.

1. Introduction

Helium nanodroplets provide a unique medium where microsolvation effects on embedded atoms and molecules can be studied at very low temperatures and in the presence of a quantum fluid.[1] It is also an environment in which a certain degree of control is available over the growth of nanodroplets and the number of embedded species. With careful choices of source and of dopant pressure it is possible to control the growth of molecular clusters from monomers to small aggregates. This offers an opportunity to study the size evolution of molecular behavior.

To date there have been relatively few studies undertaken of the fragmentation processes induced in molecules and in molecular clusters as a result of ionization following containment within a helium nanodroplet environment.[2−9] Of those studies that have been undertaken, most have been on the ionization and the fragmentation of single embedded molecules. Coupled with the prospect of charge-transfer operating as a "soft" ionization process, the nanodroplet environment holds the promise of offering a new approach to the study of ion−molecule dynamics at very low temperatures. Earlier experiments of a similar nature focused on the chemistry of molecular ions in association with small (<200 atoms) argon clusters.[10−15] From studies of the fragmentation patterns of a wide range of molecular ions, the following conclusions were drawn: (i) most ions appeared to reside on or close to the surface of a cluster; (ii) in larger clusters, molecules were ionized via a sequence of charge-transfer processes initiated from an argon ion that was generated by electron impact; (iii) those reactions that were observed occurred on a time scale of $<10^{-10}$ s. Slower processes were suppressed by competition from argon atom evaporation, which served to remove energy from the cluster; (iv) the charge-transfer mechanism did not result in soft ionization. Overall, there were marked differences between the fragmentation patterns of isolated ions and those observed when the same ions were attached to argon clusters.

The ionization of helium nanodroplets and the charge-transfer mechanism believed to be responsible for the appearance of molecular ions have been discussed in detail by Toennies and co-workers[16,17] and by Janda et al.[18,19] Ionization is assumed to be initiated via electron impact on a single He atom at or near the surface of a nanodroplet. The positive charge then delocalizes by a process of resonant charge hopping to terminate either as He_2^+, when the ionized atom combines with a neutral atom, or as a molecular ion, when He^+ collides with a molecule, thereby leading to charge-transfer. Any excess energy then evaporates the remaining helium atoms to leave a bare molecular ion.[20] It would appear that large molecular ions have sufficient heat capacity to evaporate all the helium atoms, but smaller diatomic and triatomic ions often retain several helium atoms and appear in mass spectra as M^+He_N.

Studies of the ionization energies of helium nanodroplets doped with SF_6[21] and argon clusters[22] show that the threshold for this process is 24.6 eV, which is consistent with the energy required for the production of He^+. The charge hopping process is influenced by the electrostatic potential within the doped cluster, and the positive charge is expected to move toward the center, with approximately 10 transfers occurring before the formation of either He_2^+ or a molecular ion.[19] It can be seen that, while the ionization cross-section of a droplet may increase with size, the charge hopping mechanism appears to restrict the distance a charge can move before it becomes localized. Therefore, as the nanodroplets increase in size, the probability of a dopant molecule becoming ionized may reach a maximum, after which it could begin to decline. Helium is lost from nanodroplets either after the production of He_2^+, which releases 2.35 eV of energy, or when the ionization of a molecule releases the difference between the two ionization energies as potential energy, which is an event that can boil off many thousands of atoms to leave a bare molecular ion.

† Part of the "Roger E. Miller Memorial Issue".

* E-mail: anthony.stace@nottingham.ac.uk.

10.1021/jp0713965 CCC: $37.00
Published on Web 06/22/2007

Experiments have shown[19] that the production of He_2^+ is independent of cluster size, which would not be entirely consistent with a mechanism that proposes evaporative release of a bare ion. Other explanations for the production of small ion fragments[23] involve the fission of a cluster into two or more fragments with one retaining the charge or the ejection of an ion core directly out from a helium nanodroplet. In this theory, a hot layer is formed that separates the ion fragment and allows it to leave before the dissipation of excess energy by evaporation. Farnik and Toennies[5] produced supporting evidence for this mechanism where, following the breaking of chemical bonds, small fission products, such as CH_3^+ and D^+, were observed with helium atoms attached. The same group also observed that for a number of small dopant molecules, such as Xe, NO, N_2O, SO_2, and CO_2, both the bare ions and those with helium atoms attached could be detected.

Complications in the interpretation of molecular and cluster ion fragment patterns arise because the number of embedded molecules varies according to the size (collision cross-section) of the helium droplet,[24] and because the beams are not monodispersed, a distribution consisting of empty, singly, and multiply doped nanodroplets will be present in any experiment. It has been reported by several groups that changes in ion fragmentation patterns show a clear influence through association with nanodroplets[6,7] and processes such as caging[25] and the formation of a solvation layer surrounding a molecule can affect behavior. It has also been suggested that the charge hopping process leading to ionization may depend on the nature of the solvated species.[8]

In the work reported here we have examined the fragmentation patterns of a number of single molecular ions and ion clusters trapped in helium nanodroplets. The ion clusters have all been the subject of earlier studies as isolated species, and the purpose here is to identify and characterize changes in behavior that may occur as a result of ionization being initiated in a helium nanodroplet. In addition, two single molecule systems have been studied; in the first system the precursor ion is unstable when generated in the gas phase, and in the second system, association with helium appears to have a profound effect on the fragmentation pattern. Several of the alcohols discussed here have been the subject of two earlier studies in helium nanodroplets by Yang et al.[6,9] However, the techniques used in this study to process the raw data reveal new features associated with the behavior of these particular ion clusters when trapped in helium.

2. Experimental Section

A continuous beam of helium nanodroplets was produced by the supersonic expansion of ultrapure helium (99.9999%) through a 5 mm orifice at an inlet pressure of 20 bar. The gas was precooled to ~12 K by a two-stage cryogenic system (ADP Cryogenics Inc.), which resulted in an average droplet size of $\sim 10^4$ atoms. The beam was collimated by a 0.5 mm skimmer (Beam Dynamics) and entered a 9 cm long pickup cell containing a gas-phase sample of the chemical of interest. The dopant gas pressure was maintained via a continuous, controlled flow of vapor into the cell from an external containment vessel, and molecules become embedded within the nanodroplets via collisions with the helium beam.

The doped droplet beam was further collimated by a 2 mm skimmer before entering the detection chamber, which housed a quadrupole mass spectrometer (ABB Extrel Inc.) capable of sampling either the entire mass distribution over a specified range or the intensity of a single ion at a specific *m*/*z* as a function of time. The doped nanodroplets were ionized by electron impact ionization, with the quadrupole typically operated at electron energies of 70 eV, which permitted direct comparison with analogous gas-phase studies. Although no direct measurement of the droplet size distribution has been made in these experiments, it is assumed that it follows a log-normal distribution as measured by Toennies et al.[26] and that, through scaling relationships, an average nanodroplet size can be calculated as a function of nozzle diameter, temperature, and backing pressure. The number distribution of molecules captured during the passage of a droplet though the pickup region is assumed to obey Poisson statistics.

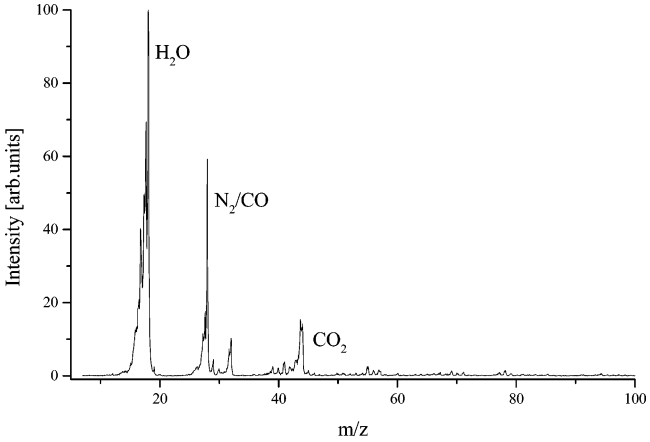

Figure 1. Mass spectrum of background gas at a pressure of 4.2×10^{-6} mbar. The mass spectrum was recorded under typical operation conditions for the experiment but with the droplet beam deflected away from the mass spectrometer.

For each molecule, mass spectra were recorded over a range of pickup cell pressures. To process the data, four mass spectra were separately recorded at each of the following steps: (i) a pure droplet beam spectrum, (ii) a mass spectrum of the background gas with the helium droplet beam turned away from the axis of the experiment, (iii) a doped nanodroplet mass spectrum, and (iv) a background mass spectrum but recorded at the same cell pressure as (iii). An example of the latter is shown in Figure 1.

Subtracting (ii) from (i) removes the ambient background, which consists mainly of H_2O, N_2, and CO_2; (iii) minus (iv) removes the interference from dopant molecules effusing from the pickup cell into the mass spectrometer. Finally, the difference between these two subtracted mass spectra removes all of those helium ion peaks not associated with the dopant molecule or its fragmentation products. Figure 2 shows how effective the procedure is in projecting out water clusters formed in helium nanodroplets. What proved more difficult to eliminate was the interference from clusters that included one or more of the above identified background molecules. In particular, water and nitrogen were found to have features in several of the mass spectra; the former was observed because of its presence on the walls of the vacuum chamber, and the latter often entered the system with the sample. Although degassing procedures were used, the pick-up processes have such a large cross-section that, at high cell pressures, small numbers of ions, including nitrogen and the nitrogen dimer associated with one or two helium atoms, appeared quite frequently.

Pressures were monitored using ion gauges sequentially positioned throughout the experiment. No direct measure of the pickup cell pressure was available; however, it was possible to deduce a (corrected) value via readings from an ion gauge situated close to the exit and corrections for gas conductance,

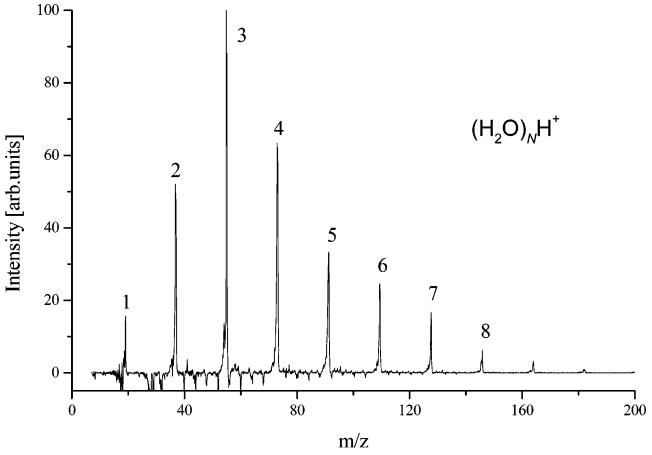

Figure 2. Mass spectrum of water in helium nanodroplets at a (corrected) pick-up cell pressure of 4.2×10^{-6} mbar. The profile matches that of a Poisson distribution, with the ion clusters ($(H_2O)_NH^+$) originating from a neutral distribution $(H_2O)_M$ ($M>N$) ionized in the helium nanodroplets.

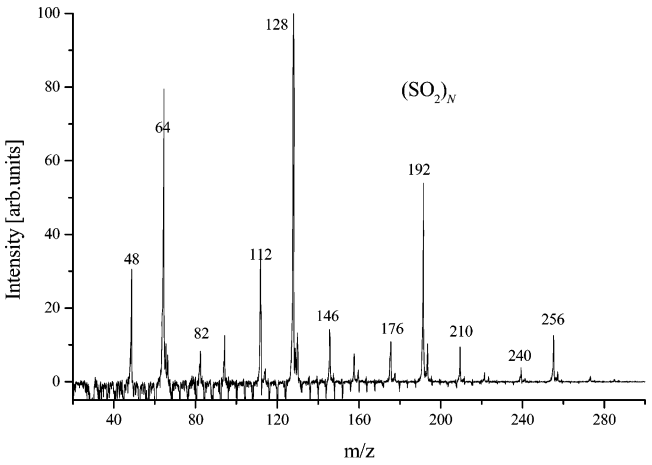

Figure 3. Mass spectrum recorded following electron impact ionization of sulfur dioxide clusters in helium nanodroplets at a pick-up cell pressure of 7.18×10^{-6} mbar.

pumping speed, and the throughput of material. It is assumed in all cases that immediately prior to ionization the ambient temperature of the embedded species is equivalent to that of the helium droplet, ~0.4 K.[27] With the exception of a few studies[28−30] where small fixed numbers of molecules are lost from clusters of a particular size, it has been found that increasing the size of a cluster beyond the dimer does not generally introduce new fragmentation pathways.

3. Results and Discussion

3.1. Sulfur Dioxide Clusters, $(SO_2)_N$. Figure 3 shows a cluster mass spectrum and the accompanying fragmentation products resulting from the ionization of helium nanodroplets doped with sulfur dioxide. The most intense ions appear at $m/z = 64$, 128, and 192, and can be attributed to SO_2^+, $(SO_2)_2^+$, and $(SO_2)_3^+$, respectively. There are some important differences between what is shown in Figure 3 and in the photoionization mass spectra of SO_2 clusters as reported by Knappenberger and Castleman.[31] Both S^+ and O_2^+ are missing from the droplet mass spectra, but they are clearly seen following the photoionization of SO_2 clusters.[31] The absence of these ions is not on the grounds of energetics, because with appearance energies of 17.5 eV for O_2^+ and 16.5 eV for S^+ [32], these values are well below the threshold energy available from He^+ charge-transfer.

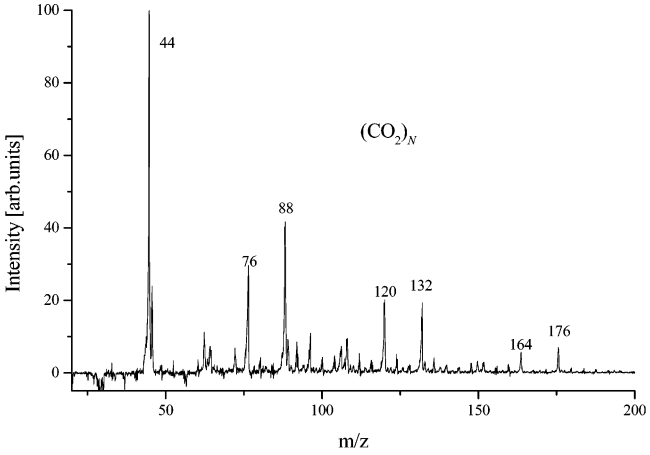

Figure 4. Mass spectrum recorded following the ionization of carbon dioxide clusters in helium nanodroplets at a pick-up cell pressure of 6.4×10^{-6} mbar.

However, it is quite possible that the amount of energy that ions receive from the latter process is less than that available from photoionization with femtosecond laser pulses. Further support for this suggestion is provided below.

In terms of the energy available to SO_2 clusters for ionization and reactivity, the most appropriate comparison with other experiments comes from the recent work of Dong et al.[33] They used single photons with an energy of 26.5 eV to photoionize SO_2 clusters, and the relative intensities they report[33] [$(SO_2)_N^+ > (SO_2)_NSO^+$] are very similar to those shown in Figure 3. However, both are quite different from the results presented by Knappenberger and Castleman,[31] whose mass spectra show the fragment ions to be more intense than the precursors. Again, this observation would suggest that the energy available from He^+ charge-transfer is less than that ions receive via femtosecond photoionization.

Further comparisons can be made with the work of Dong et al.[33] through their experiments on SO_2^+ in association with water. The presence of trace amounts of H_2O in the pick-up zone (cell + flight path) means that some SO_2 cluster ions are formed as $(SO_2)_NH_2O^+$. These can clearly be seen at $m/z = 82$, 146, and 210 in Figure 3, and possible reaction products can also be identified; the ion seen at $m/z = 65$ could be SO_2H^+ and that at $m/z = 66$ could be either $SO_2H_2^+$ or SOH_2O^+.

3.2. Carbon Dioxide Clusters, $(CO_2)_N$. A typical mass spectrum recorded from the presence of carbon dioxide molecules trapped in helium nanodroplets is shown in Figure 4. The most intense ion at $m/z = 44$ is assigned to CO_2^+, with the pick-up of additional molecules giving rise to cluster formation and with an ion pattern represented by the series $(CO_2)_N^+$ at $m/z = 88$, 132, and 176 for $N = 2$, 3, and 4, respectively. In previous studies of the chemistry of CO_2^+ cluster ions, the fragment ions $(CO_2)_NO^+$, $(CO_2)_NO_2^+$, and $(CO_2)_NCO^+$ have appeared in the mass spectra.[34,35] A comparison with Figure 4 shows only one of these to be present with any significant intensity, and that is $(CO_2)_NO_2^+$ for $N = 1$, 2, and 3. The mechanism proposed by Romanowski and Wanezek[34] to account for the appearance of $(CO_2)_NO_2^+$ fragmentations involves the following two-step ion molecule reaction:

$$(CO_2)_N^+ \rightarrow (CO_2)_{(N-1)}O^+ + CO \quad (1)$$

$$(CO_2)_{(N-1)}O^+ \rightarrow (CO_2)_{(N-2)}O_2^+ + CO \quad (2)$$

This mechanism is based on existing evidence from gas-phase ion−molecule reactions and is proposed on the grounds that a

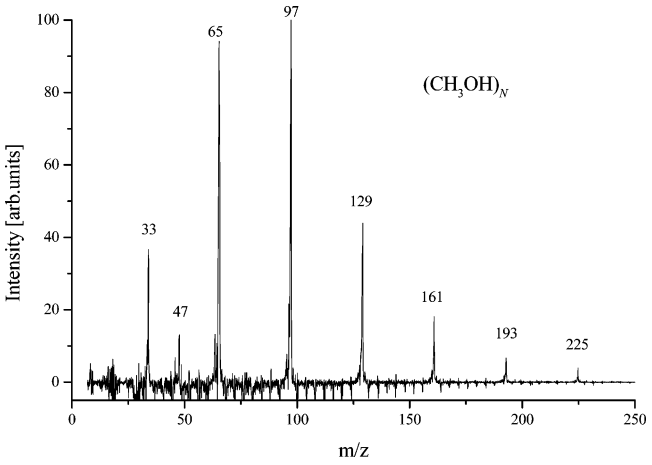

Figure 5. Mass spectrum recorded following the electron impact ionization of methanol clusters in helium nanodroplets at a pick-up cell pressure of 3.12×10^{-6} mbar.

direct reaction of the type shown in eq 3 is energetically unfavorable.[34]

$$(CO_2)_N^+ \rightarrow (CO_2)_{(N-1)}O_2^+ + C \quad (3)$$

The preparation of $(CO_2)_N^+$ cluster ions by SIMS does give $(CO_2)_{(N-1)}C^+$ as one of the fragment, and this probably reflects the high energies available in such experiments.[36] If $(CO_2)_{(N-1)}O_2^+$ was generated via eqs 1 and 2, then the appearance of $(CO_2)_{(N-1)}O^+$ as a fragment ion might have been expected. The alternatives are either a direct, high-energy reaction (i.e., step (3)), or that O_2 is present as an impurity through air leaked into the pick-up cell. However, if the latter were happening, then peaks in the form of $(CO_2)_N N_2^+$ would be expected to be even more prominent than those containing O_2. Given the energy available from He^+ charge-transfer, the most probable outcome would appear to be eq 3, the direct high-energy reaction pathway.

3.3. Methanol Clusters, $(CH_3OH)_N$. As in the case for water clusters, the ionization of bare neutral methanol clusters, $(CH_3OH)_N$, typically leads to the formation of protonated ions via the reaction shown in eq 4.[37]

$$(ROH)_N + e \rightarrow (ROH)_{N-M-1}H^+ + (ROH)_M \cdot RO + 2e \quad (4)$$

Consistent with this mechanism and with other EI spectra,[38−41] protonated cluster ions dominate the mass spectra generated from methanol clusters trapped in helium nanodroplets,[7] and a typical example is shown in Figure 5. In contrast with previously reported gas-phase spectra, no peak corresponding to the precursor ion (CH_3OH^+) is seen, and there is no evidence of the series $(CH_3OH)_N(H_2O)H^+$. However, these latter ions are not typically observed until $N > 6$, and so the low intensity of higher-order cluster ions may contribute to this absence.[42]

Although the distribution of intensities of the $(CH_3OH)_NH^+$ ions appears to follow a Poisson distribution, the ion at $N = 3$ does have an anomalously high intensity. This apparent "magic number" is consistent with previous gas-phase photoionization experiments by El-Shall et al.,[40] who proposed that protonated methanol ion can form a stable hydrogen-bonded complex with two other neutral precursor molecules. One further feature of note in Figure 5 is the appearance of a peak at $m/z = 47$, which was previously reported by Morgan and Castleman[29] and is thought to be generated via the reaction shown in eq 5.

$$(CH_3OH)_2H^+ \rightarrow (CH_3)_2OH^+ + H_2O \quad (5)$$

No evidence of H_2O loss from higher-order protonated clusters was observed in either this or the earlier helium droplet study of alcohol clusters by Yang et al.[9] However, the latter study did show the presence of ions of the form $(CH_3OH)_NH^+ \cdot H_2O$, but as suggested by the authors, these could arise from the pick-up of neutral water molecules by the helium droplets.

3.4. Ethanol Clusters, $(C_2H_5OH)_N$. A typical mass spectrum recorded from neutral ethanol clusters in helium nanodroplets is presented in Figure 6. Similar to the previous example for methanol, the spectrum is dominated by the presence of protonated ethanol clusters, $(CH_3CH_2O)_NH^+$, corresponding to ions seen at $m/z = 47$, 93, 139, etc. (for $N = 1$, 2, 3, etc.). In addition, there are fragment ions that are assumed to arise from the reactions shown in eqs 6−8:

$$(CH_3CH_2OH)_N^+ \rightarrow (CH_3CH_2OH)_{N-1}(CH_3CHOH)^+ + H \quad (6)$$

$$(CH_3CH_2OH)_N^+ \rightarrow (CH_3CH_2OH)_{N-1}CH_2OH^+ + CH_3 \quad (7)$$

$$(CH_3CH_2OH)_2H^+ \rightarrow (CH_3CH_2)_2OH^+ + H_2O \quad (8)$$

The reaction shown in eq 6 has not previously been reported in gas-phase experiments on bare protonated ethanol clusters, but in this case, it is thought to be responsible for the fragments seen at $m/z = 45$, 91, 137. This conclusion assumes that it is the unprotonated cluster that is reacting and that the product is the response of a single molecular ion to a rapid injection of energy from charge-transfer. In some respects, the −H cluster ions could be viewed as a higher energy but complementary product to the protonated clusters. Fragment ions arising from the reaction in eq 6 were also noted by Yang et al.[9]

It is known that for high molecular weight primary alcohols the precursor ion is generally a minor product of electron impact ionization and that, in the case of the lighter alcohols, the formation of an oxonium ion via C−C cleavage tends to dominate gas-phase ion fragmentation. However, in the case of ethanol in helium clusters, it has been suggested[6] that cleavage of the C−H bond at the α carbon is a more significant fragmentation channel (which leads to enhanced production of $CH_3C(H)=O^+H$ ions), and the trends reported here provide additional support for that suggestion.

The series of ions seen at $m/z = 77$, 123, etc. is attributed to the reaction shown in eq 7, where, immediately following ionization, cleavage of the α C−C bond in an ethanol molecular ion occurs. These product ions are found to be of minor importance in this study, which is in agreement with previous photoionization studies of gas-phase ethanol clusters.[40,43] An earlier study of cluster ions composed of primary alcohols larger than ethanol reported the appearance of a product ion that could be attributed to the formation of protonated aldehyde.[37] Fragments of the form $R \cdot CH_2OH^+$ (protonated ketones and aldehydes) appeared more frequently following the ionization of clusters composed of secondary and tertiary alcohols.[37]

Finally, the ion seen at $m/z = 75$ probably arises from the reaction shown in eq 8; however, the intensity of this ion is far weaker than that observed in the gas-phase, where the loss of neutral water represents a major fragmentation channel. This reaction pathway appears to be limited to the protonated dimer, which again agrees with previous observations.[37,44]

3.5. 1-Propanol Clusters, $(C_3H_7OH)_N$. The 1-propanol spectrum presented in Figure 7 marks a distinct departure from the previous series of primary alcohols, with the overall fragment

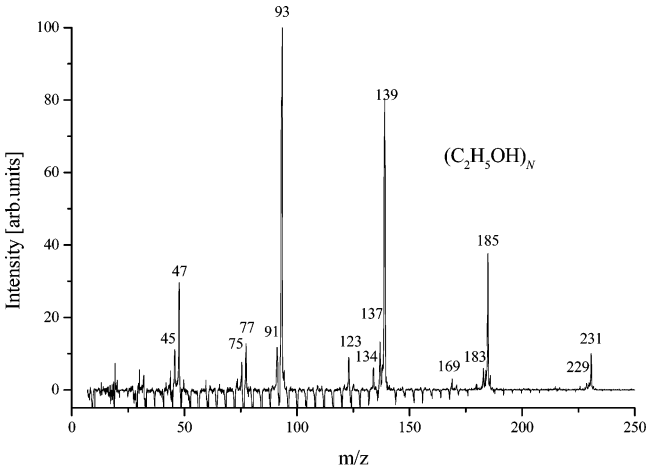

Figure 6. Mass spectrum recorded following the electron impact ionization of ethanol clusters in helium nanodroplets at a pick-up cell pressure of 5.54×10^{-6} mbar.

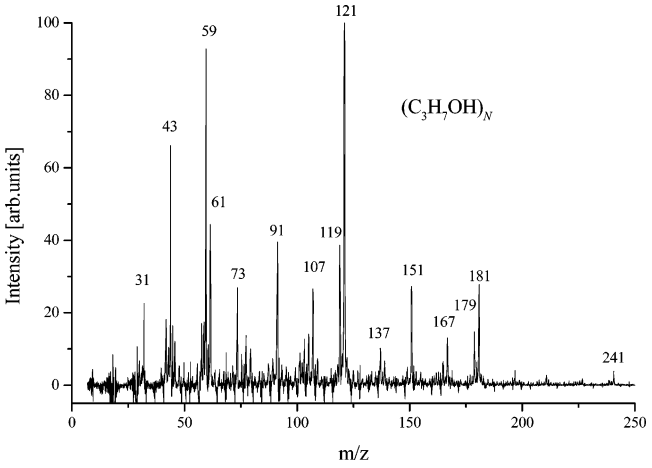

Figure 7. Mass spectrum recorded following the electron impact ionization of 1-propanol clusters in helium nanodroplets at a pick-up cell pressure of 4.87×10^{-6} mbar.

pattern appearing significantly more congested. As in the earlier experiments, the protonated cluster ions at $m/z = 61$, 121, etc., are the most prominent ions in the mass spectrum. As seen in the case of ethanol, there also is extensive loss of H, when assuming that the ion is due to H atom loss from a single molecular ion.

In the gas-phase, the dominant fragmentation pathway for the 1-propanol ion is given by the reaction shown in eq 9, below. Although the intensity of the $m/z = 31$ product ion appears to be reduced significantly in the helium droplet mass spectrum, the ion does appear to contribute to the cluster fragmentation pattern with the presence of $m/z = 91$ and 151 in the mass spectrum. Further evidence of high-energy reaction pathways is given by the presence of a strong peak at $m/z = 43$ ($C_3H_7^+$); however, this route does not extend to the larger clusters. In the absence of isotopes it is not possible to make accurate assignments to a number of the minor fragment peaks seen in Figure 7.

$$C_3H_7OH^+ \rightarrow CH_3O^+ + C_2H_5 \qquad (9)$$

A plot of the intensities of the two most prominent ions observed in the 1-propanol mass spectrum as a function of the doping pressure in the pick-up chamber is shown in Figure 8.

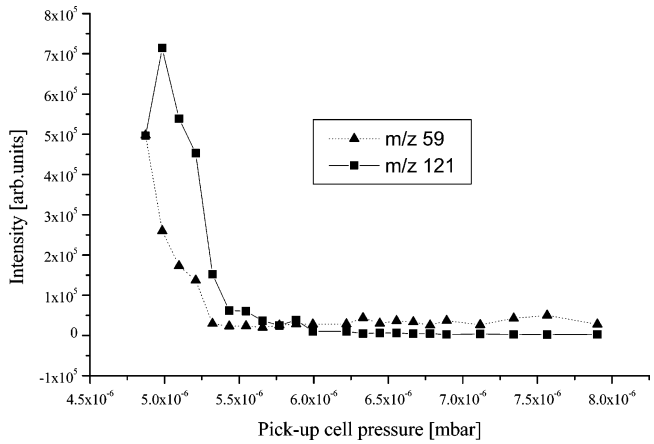

Figure 8. Ion intensities of two fragments from the ionization of 1-propanol clusters plotted as a function of gas pressure in the pick-up cell.

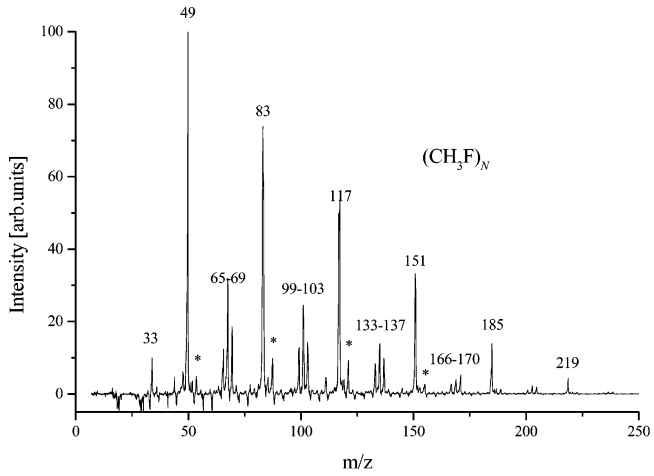

Figure 9. Mass spectrum recorded following the electron impact ionization of methyl fluoride clusters in helium nanodroplets at a corrected pick-up cell pressure of 5.2×10^{-6} mbar.

There is clearly a marked difference in behavior between the product of H atom loss ($m/z = 59$) and the protonated trimer ion ($m/z = 121$). Such behavior could reflect the different origins of the ions; if $m/z = 59$ predominantly comes from the neutral monomer, then the Poisson statistics of the pick-up process should rapidly reduce the relative intensity of that precursor as the pressure is increased. In contrast, contributions to the protonated trimer will come from neutral droplets containing four or more molecules, and the intensities of these will gradually increase as a function of the cell pressure. Eventually, the pressure in the pick-up cell becomes sufficiently high that the droplets break apart either through scattering or through extensive evaporation induced by multiple pick-ups.

3.6. Methyl Fluoride Clusters, $(CH_3F)_N$. Substituting the −OH functional group in methanol with the more electronegative fluorine atom produces a markedly different cluster ion fragmentation pattern. Dominated by cluster ion fragments, a typical mass spectrum recorded following the ionization of CH_3F clusters in helium nanodroplets is presented in Figure 9. The mass spectrum consists of a number of regular series of reaction products, many of which were previously identified by Garvey and Bernstein[45] in their study of the chemistry of bare methyl fluoride cluster ions. With reference to their results together with biomolecular ion−molecule data taken from the work of Beauchamp and co-workers,[46−48] the dominant reactions taking

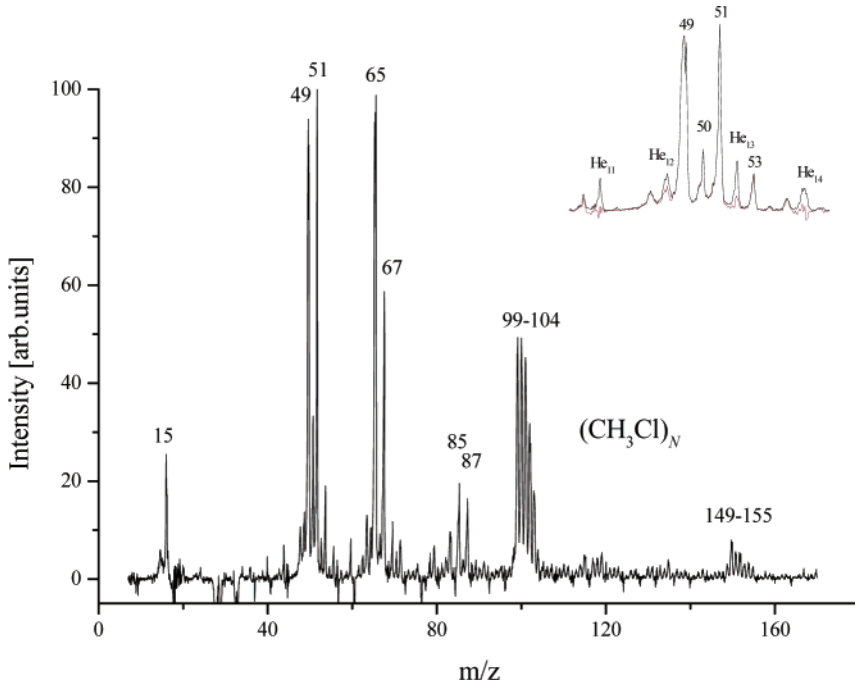

Figure 10. Mass spectrum recorded following the electron impact ionization of chloromethane clusters in helium nanodroplets at a pick-up cell pressure of 3.42×10^{-6} mbar.

place within the bare methyl fluoride cluster ions were proposed to be as follows:

$$CH_3F^+ + CH_3F \rightarrow CH_3FH^+ + CH_2F \quad (10)$$

$$CH_3FH^+ + CH_3F \rightarrow (CH_3)_2F^+ + HF \quad (11)$$

$$(CH_3)_2F^+ \rightarrow CH_2F^+ + CH_4 \quad (12)$$

Comparing the above with Figure 9, it can be seen that reaction (11) produces the most intense sequence of ions, $(CH_3F)_N$-$(CH_3)_2F^+$, which appear at $m/z = 49$, 83, 117, etc. for $N = 0$, 1, 2, etc. What is unusual, given the above mechanism, is that there are no bare CH_3FH^+ ions in Figure 9; however, there is a series starting at $m/z = 69$ that is consistent with formation of the protonated dimer and larger, protonated clusters. A single peak observed at $m/z = 33$ can be attributed to CH_2F^+, with further evidence of a cluster sequence $(CH_3F)_NCH_2F^+$ at $m/z =$ 67, 101, 135, etc. Overall, the relative intensities of the ions appear very different from those reported by Garvey and Bernstein,[45] particularly with the helium droplet spectrum being dominated by the series $(CH_3F)_N(CH_3)_2F^+$, which is not seen in the case for the bare gas-phase CH_3F^+ clusters.

The ionization energy of methyl fluoride is 12.5 eV.[46] Therefore, with 24.6 eV imparted to the dopant cluster via the charge-transfer process, there is an excess of ~12 eV that, in principle, is more than sufficient to evaporate the entire helium droplet. The gas-phase methyl fluoride spectrum shows ions at $m/z = 34$ (100%), $m/z = 33$ (90%), and $m/z = 15$ (15%), with the pathway $CH_3F^+ \rightarrow CH_2F^+ + H$ having a barrier of just 1 eV. In their experiments on the ion molecule chemistry of CH_3F^+, Blint et al.[48] noted that for eq 12 to proceed the precursor $(CH_3)_2F^+$ must be vibrationally excited and that the product (CH_2F^+) then remains inert toward further reactivity with CH_3F. Rather than participating in eq 10−12, the formation of several of the fragments via direct bond-breaking would appear to offer a more satisfactory explanation than the ion−molecule routes given above. Fission processes would account for the isolated ion seen at $m/z = 33$ when all other reaction products are in the form of clusters. It would also overcome the requirement that the precursor in eq 12 retain vibrational energy at the ambient temperature (0.38 K) of the nanodroplets. The unreactive nature of CH_2F^+ would account for its continued appearance in larger clusters. In a similar vein, the product ion $(CH_3)_2F^+$ could be re-expressed as $(CH_3F)CH_3^+$ and be taken as the product of C−F bond fission.

Two further series of ions warrant some discussion. The first, at $m/z = 65$, 99, 133, etc., is of low intensity and is attributed by Garvey and Bernstein to the loss of F_2 from $(CH_3F)_N^+$ cluster ions. In the alternative scheme discussed above, the ions could come from the sequential loss of F. The second series, marked by * in Figure 9, corresponds to either $(CH_3F)_NF^+$ or $(CH_3F)_{N-1}(CH_3)_2F^+He$ cluster ions. The fact that helium does not appear to attach itself to any other fragments would favor $(CH_3F)_NF^+$, which could again be seen as the high-energy complement to CH_3^+. The high appearance energy of F^+ means that the ion is absent from the gas-phase mass spectrum of CH_3F and its clusters.[45]

3.7. Chloromethane Clusters, $(CH_3Cl)_N$. Figure 10 shows a processed mass spectrum recorded for CH_3Cl embedded in helium nanodroplets. Interpretation of the mass spectrum is made more challenging by the presence of the two chlorine isotopes ^{37}Cl and ^{35}Cl; therefore, this analysis focuses on the behavior of small clusters ions. A complement to these experiments is an earlier study by Garvey and Bernstein of the bare cluster ions.[49]

There are certain similarities with the chemical processes as seen for the methyl fluoride ion, but there are also considerable differences in the relative intensities of the respective fragments. The ions seen at $m/z = 49$ and 51 correspond to CH_2Cl; their high intensities suggest a more facile fragmentation pathway than that seen for CH_3F. The inset shows an expanded view of this region of the mass spectrum, from which it can be seen that there is minimal evidence of the precursor ions ($m/z = 50$ and 52). The peaks seen at $m/z = 15$ and 65/67 represent the only real evidence of a fragment series, which corresponds to $(CH_3Cl)_NCH_3^+$ for $N = 0$ and 1. There is some evidence for an

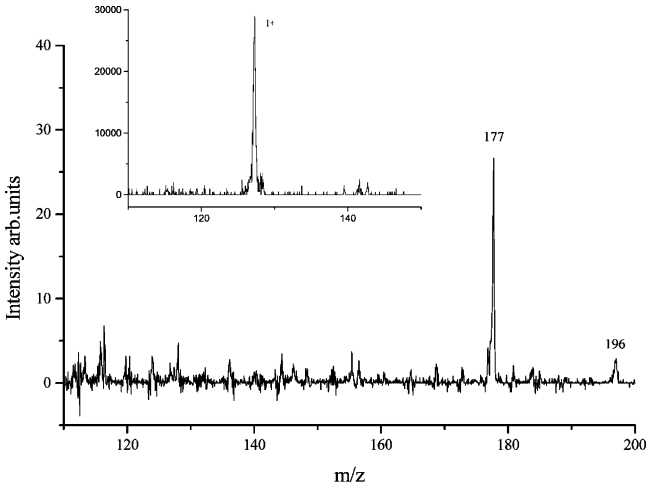

Figure 11. Mass spectrum recorded following the electron impact ionization of single trifuoroiodomethane molecules in helium nanodroplets at a pick-up cell pressure of 5.9×10^{-6} mbar. Inset: section of a gas-phase mass spectrum recorded from molecules drifting out from the pick-up cell while the helium beam was aligned off-axis to the detector.

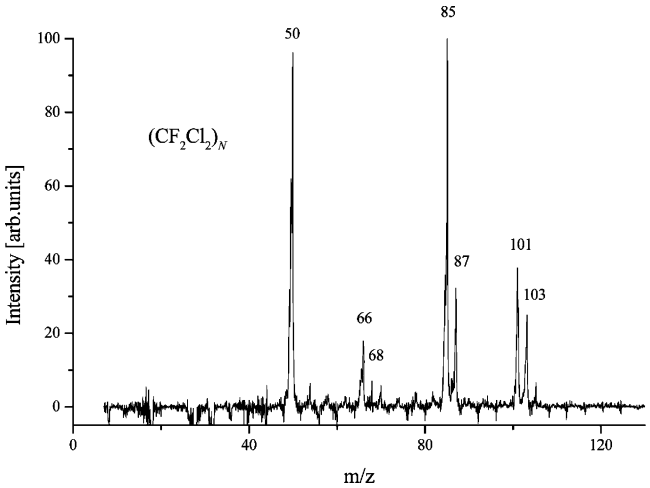

Figure 12. Mass spectrum recorded following the electron impact ionization of single dichlorodifluoromethane molecules in helium nanodroplets at a pick-up cell pressure of 2.71×10^{-6}mbar.

$N = 2$ component at $m/z \sim 118$, but the intensities are low. The relative intensities of the fragment ions appearing at $m/z = 65/67$ are considerably higher than those reported by Garvey and Bernstein, which suggests that in these experiments more energy is available to promote bond fission. It is noteworthy that many of the isotopic ratios do not match the expected values; whereas it is known that low temperatures can lead to isotope fractionation,[50] this would seem unlikely here given that the initial internal energy of a molecular ion in a droplet could be as high as 12 eV. An alternative possibility is that fractionation could occur via selective evaporation from cold fragments that remain after the helium atoms are lost.

3.8. Trifluoroiodomethane Molecule, CF_3I. The most significant result observed for this molecule occurred when, on average, just a single ion was trapped in a helium droplet, and the most relevant section of a mass spectrum recorded under such conditions is shown in Figure 11. The gas-phase mass spectrum of CF_3I is dominated by the precursor ion at $m/z = 196$ (CF_3I^+) and a fragment at $m/z = 127$, which is I^+. In complete contrast, Figure 11 shows the precursor ion at <5% of the ion with maximum intensity (CF_2I^+), and the I^+ ion is missing completely from the mass spectrum. Although I^+ is apparent as a very weak signal in the raw, unprocessed spectra, it can be shown that this intensity derives entirely from background drift. This effect is demonstrated in the inset to Figure 11, where CF_3I has been allowed to drift out from the pick-up cell in the absence of the nanodroplet beam. As can be seen, a strong I^+ signal appears when isolated CF_3I molecules are ionized. The barrier to production of I^+ from CF_3I^+ is 3 eV; however, the fact that CF^+ (not shown) appears in the helium droplet mass spectra and has a higher appearance energy than I^+ would suggest that the energy available from charge-transfer is not the limiting factor in this process.

One possible explanation of events taking place when CF_3I is ionized in helium nanodroplets is that the molecule is first ionized by charged-transfer from He^+, with the difference in ionization energies between the two species remaining available for fragmentation and evaporation of helium atoms. The weakest bond (C−I) is then broken, which leads to the charge becoming localized on the fragment with the lowest ionization energy, which is CF_3.[51] Such a process might be aided by the dipole steering process identified by Lewis et al.,[8] which would result in He^+ colliding with the CF_3 end of the molecule. Very rapid fragmentation would then yield CF_3^+ with little or no opportunity for curve crossing to give I^+. CF_3^+ (not shown) is a prominent fragment in the droplet mass spectrum.

In terms of the dominant fragment (CF_2I^+) shown in Figure 11, it should be noted that the most recent photoionization measurements by Powis et al.[52] report the appearance energy of this ion as having the same value as I^+ (13.4 eV). Therefore, it is quite possible that the preference for CF_2I^+ is also influenced by the dipole steering process and that the positive charge on the part of the molecular ion that is subject to the initial ionization process is localized via solvation by the surrounding helium atoms.

3.9. Dichlorodifluoromethane Molecule CCl_2F_2. The mass spectrum shown in Figure 12 represents a typical processed mass spectrum recorded for dichlorodifluoromethane (Freon 12) in helium nanodroplets. Calculations by Afosimov et al.[53] show the most facile fragmentation pathways to be those shown in eqs 13 and 14:

$$CF_2Cl_2^+ \rightarrow CF_2Cl^+ + Cl \quad (13)$$

$$CF_2Cl_2^+ \rightarrow CFCl_2^+ + F \quad (14)$$

The precursor ion ($CF_2Cl_2^+$) is calculated to be unstable with respect to reaction (13) by 1.53 eV; this would account for the ion, which should appear at $m/z = 120-124$, being absent from Figure 12. In contrast, eq 14 is calculated to have a barrier, which could account for its product ($CFCl_2^+$, $m/z = 101-105$) having a lower intensity than CF_2Cl^+ ($m/z = 85-87$) from eq 13. In fact, both fragment ions emerge from the helium nanodroplets with intensities comparable to those seen in gas-phase mass spectra, which is not the case for many of the molecular ions examined in this study. Surprisingly, the second most intense ion from the helium nanodroplets (96% of the intensity of the most prominent ion) is found at $m/z = 50$ and is the product of eq 15:

$$CF_2Cl^+ \rightarrow CF_2^+ + Cl \quad (15)$$

Given that the calculations show this pathway to have a barrier of 3.27 eV, it is perhaps surprising that CF_2^+ should appear with the intensity seen in Figure 12. The calculations of Afosimov et al.[53] suggest that Cl^+ and F^+ should arise from the fragmentation of metastable states of the precursor ion. With

reaction barriers comparable to that which leads to the appearance of CF_2^+, the absence of both Cl^+ and F^+ suggests that the necessary metastable states are not being created as a result of charge-transfer.

Conclusion

A number of molecules and clusters were trapped in helium nanodroplets, and their ion chemistry was observed following electron impact ionization. In most examples, the fragment ions and/or their relative intensities are quite different from those seen when either the clusters or the molecular ions are studied in isolation. Many of the reaction products can be accounted for through bond fission processes rather than the ion−molecule reactions that have previously been used to interpret data on the isolated ions. It would appear that the charge-transfer route to molecular ionization, which proceeds via charge-exchange from He^+, does not offer a soft route to the formation of low-energy ions.

Acknowledgment. The authors would like to thank EPSRC for financial support and for the award of research studentships to A.B. and J.J. The authors would also like to thank Dr. B. J. Duncombe for proposing several of the molecular systems studied in this work.

References and Notes

(1) Toennies, J. P.; Vilesov, A. F. *Angew. Chem., Int. Ed.* **2004**, *43*, 2622.
(2) Peterka, D. S.; Kim, J. H.; Wang, C. C.; Neumark, D. M. *J. Phys. Chem. B* **2006**, *110*, 19945.
(3) Lewis, W. K.; Applegate, B. E.; Sztáray, J.; Sztáray, B.; Baer, T.; Bemish, R. J.; Miller, R. E. *J. Am. Chem. Soc.* **2003**, *126*, 11283.
(4) Lewis, W. K.; Bemish, R. J.; Miller, R. E. *J. Chem. Phys.* **2005**, *123*, 141103.
(5) Fárnik, M.; Toennies, J. P. *J. Chem. Phys*. **2005**, *122*, 014307.
(6) Yang, S.; Brereton, S. M.; Wheeler, M. D.; Ellis, A. M. *Phys. Chem. Chem. Phys*. **2005**, *7*, 4082.
(7) Yang, S.; Brereton, S. M.; Wheeler, M. D.; Ellis, A. M. *J. Phys. Chem*. **2006**, *110*, 1791.
(8) Lewis, W. K.; Lindsay, C. M.; Bemish, R. J.; Miller, R. E. *J. Am. Chem. Soc*. **2004**, *127*, 7235.
(9) Yang, S.; Brereton, S. M.; Ellis, A. M. *Int. J. Mass Spectrom* **2006**, *253*, 79.
(10) Stace, A. J. *Chem. Phys. Lett*. **1983**, *99*, 470.
(11) Stace, A. J. *J. Phys. Chem.* **1983**, *87*, 2286.
(12) Stace, A. J. *J. Am. Chem. Soc.* **1984**, *106*, 4380.
(13) Stace, A. J. *J. Am. Chem. Soc.* **1985**, *107*, 755.
(14) Stace, A. J. *J. Phys. Chem.* **1987**, *91*, 1509.
(15) Bernard, D. M.; Gotts, N. G.; Stace, A. J. *Int. J. Mass Spectrom. Ion Processes* **1990**, *95*, 327.
(16) Scheidemann, A.; Schilling, B.; Toennies, J. P. *J. Phys. Chem*. **1993**, *97*, 2128.
(17) Lewerenz, M., B.; Schilling, B.; Toennies, J. P. *Chem. Phys. Lett*. **1993**, *206*, 381.
(18) Callicoatt, B. E.; Mar, D. D.; Apkarian, V. A.; Janda K. C. *J. Chem. Phys*. **1996**, *105*, 7872.
(19) Callicoatt, B. E.; Förde, K.; Jung, L. F.; Ruchti, T.; Janda, K. C. *J. Chem. Phys*. **1998**, *109*, 10195.
(20) Atkins, K. R. In *Proceedings of the International School of Physics Enrico Fermi, Course XXI on Liquid Helium*; Carerei, G. Ed.; Academic; New York, 1963, 403.
(21) Scheidemann, A.; Schilling, B.; Toennies, J. P. *J. Phys. Chem*. **1993**, *97*, 2128.
(22) Callicoatt, B. E.; Förde, K.; Ruchti, T.; Jung, L. F.; Janda, K. C.; Halberstadt, *J. Chem. Phys*. **1998**, *108*, 9371.
(23) Gspann, J.; Vollmar, H. *J. Low Temp. Phys.* **1981**, *45*, 343.
(24) Lewerenz, M.; Schilling, M.; Toennies, J. P. *J. Chem. Phys*. **1995**, *102*, 8191.
(25) Nakayama, A.; Yamatahita, K. *J. Chem. Phys.* **2000**, *82*, 4076.
(26) Lewerenz, M.; Schilling, B.; Toennies, J. P. *Chem. Phys. Lett*. **1993**, *206*, 381.
(27) Lewerenz, M.; Schilling, B.; Toennies, J. P. *Phys. Rev. Lett*. **1995**, *75*, 1566.,
(28) Begemann, W.; Meiwes-Broer, K. H.; Lutz, H. O. *Phys. Rev. Lett.* **1986**, *56*, 2248.
(29) Echt, O.; Dao, P. D.; Morgan, S.; Castlemann, A. W. *J. Chem. Phys*. **1985**, *82*, 4076.
(30) Winkel, J. F.; Stace, A. J. *Chem. Phys. Lett.* **1994**, *221*, 431.
(31) Knappenberger, K. L.; Castleman, A. W. *J. Chem. Phys*. **2004**, *121*, 3540.
(32) NIST Chemistry WebBook. http://webbook.nist.gov/chemistry.
(33) Dong, F.; Heinbuch, S.; Rocca, J. J.; Bernstein, E. R. *J. Chem. Phys.* **2006**, *125* 154317.
(34) Romanowski, G.; Wanczek, K. P. *Int. J. Mass Spectrom. Ion Processes* **1984**, *62*, 277.
(35) Stamatovic, A.; Stephan, K.; Mark, T. D. *Int. J. Mass Spectrom. Ion Processes* **1985**, *63*, 37.
(36) Orth, R. G.; Jonkman, H. T.; Michl, J. *J. Am. Chem. Soc.* **1981**, *103*, 1564.
(37) Shukla, A. K.; Stace, A. J. *J. Phys. Chem*. **1992**, *92*, 2579.
(38) Vaidyanathan, G.; Collbaugh, M. T.; Peifer, W. R.; Garvey, J. F. *J. Chem. Phys*. **1991**, *94*, 1850.
(39) Morgan, S.; Castleman, A. W. *J. Am. Chem. Soc*. **1987**, *109*. 2867.
(40) EI-Shall, M. S.; Marks, C.; Sieck, L. W.; Moet-Ner, M. *J. Phys. Chem*. **1992**, *96*, 2045.
(41) Morgan, S.; Castleman, A. W. *J. Phys. Chem.* **1989**, *93*, 4544.
(42) Dong, F.; Heinbuch, S.; Rocca, J. J.; Bernstein, E. R. *J. Chem. Phys.* **2006**, *124*, 224319.
(43) Tsai, S. T.; Jiang, J. C.; Lin, M. F.; Lee, Y. T.; Ni, C. H. *J. Chem. Phys*. **2004**, *120*, 8979.
(44) Bomse, D. S.; Beauchamp, J. L. *J. Am. Chem. Soc*. **1981**, *103*, 3292.
(45) Garvey, J. F.; Bernstein, R. B. *Chem. Phys. Lett.* **1986**, *126*, 395.
(46) McMahon, T. B.; Blint, R. J.; Ridge, D. P.; Beauchamp, J. L. *J. Am. Chem. Soc*. **1974**, *94*, 8934.
(47) Beauchamp, J. L.; Holtz, D.; Woodgate, S. D.; Patt, S. L. *J. Am. Chem. Soc*. **1972**, *94*, 2798.
(48) Blint, R. J.; McMahon, T. B.; Beauchamp, J. L. *J. Am. Chem. Soc*. **1974**, *96*, 1269.
(49) Garvey, J. F.; Bernstein, R. B. *J. Phys*. *Chem.* **1986**, *90*, 3577.
(50) Calado, J. C. G.; Lopes, J. N. C.; Nunes da Ponte, M.; Rebelo, L. P. N. *J. Chem. Phys.* **1997**, *106*, 8792.
(51) Garcia, G. A.; Guyon, P.-M.; Powis, I. *J. Phys. Chem.* **2001**, *105*, 8296.
(52) Powis, I.; Dutuit, O.; Richard-Viard, M.; Guyon, P. M. *J. Chem. Phys*. **1990**, *92*, 1643.
(53) Afrosimov, V. V.; Basalaev, A. A.; Fastrup, B.; Hordal-Pedersen, E.; Panov, M. N.; Tulub, A. V.; Yakovlev, D. S. *J. Phys. B: At., Mol. Opt. Phys*. **2003**, *36*, 1991.